JOURNAL PUNJAB ACADEMY OF SCIENCES (Peer Reviewed Open Access Journal)
JPAS, 22: 41-52 (January-December, 2022)
Available online at www.jpas.in
ISSN 2229-7014 (P)

THICKNESS MEASUREMENTS OF MULTI-LAYER SAMPLES USING PHOTON-ATOM INTERACTIONS IN X-RAY ENERGY REGION

V. Singh[1], Kailash[2], J.S. Shahi[2] and D. Mehta[2,*]
[1]Sri Guru Gobind Singh College, Sector-26, Chandigarh-160019, India
[2]Department of Physics, Panjab University, Chandigarh-160014, India
*Corresponding author's Email: dmehta@pu.ac.in

ABSTRACT

The present work reports a method for thickness measurements of multi-layer samples using energy dispersive photon-atom interaction setup involving 59.5 keV γ-rays from ^{241}Am radioactive source. The inelastic information has been used to measure thickness of polymer (mylar/polypropylene) films over a wide range 100 μg/cm^2 - 600 mg/cm^2 (~700 - 4200,000 Å). The setup can be further improved for lower thickness ~few Å using in-vacuo measurements involving low-energy photons ~10 keV. The measurements were also extended to determine thickness of different layers of Cu and Pb-Sn alloy foils sandwiched between polymer films using the characteristic x-ray, elastic- and inelastic-scattering information. The experimental results recommend the use of reported methodology for thickness measurement of low-Z materials deposited on a thick substrate for material characterization. Various aspects of interaction of X-ray photons (below ~100 keV) with matter, i.e., about characteristic X-ray photons, elastic- and inelastic-scattered photons have been discussed for the sample elemental/thickness analysis applications.

Keywords: Photon-atom interaction, multilayer samples, thickness, X-rays, energy-dispersive X-ray detection

INTRODUCTION

Non-destructive determination of thickness of different layers in a multilayer sample or thin film fabricated on thick substrate is important in material science research samples and also in the furnished industrial products. Most of the experimental techniques used for thickness determination involve measurements of resistance, capacitance, inductance, optical signals and interaction of ionizing radiations (α, β and γ/X-rays) with film materials [Gardener *et al*. (2004), Hobbis and Aruleswaran (2005), Ebel *et al*. (1999), Rajesh *et al.* (2017), Hussein (2003), Lhotka *et al.* (2001)]. Rutherford backscattering (RBS) [Ribeiro *et al*. (2019), Draxler *et al.* (2002)] and Elastic recoil detection analysis (ERDA) [Suzukia *et al.* (2020)] measurements using proton or heavier ion beams from accelerators are used to obtain elemental concentration/depth profiles in multilayer thin films. Energy-loss measurements of alpha particles from radioactive decays can be used to determine thickness and uniformity of the self-supporting thin films and requires precise knowledge of energy loss curves for different elements or good calibration standards. Under harsh industrial conditions, the γ/X-ray based techniques are beneficial as compared to non-

radiation based methods to measure the thickness of thin layers [Sowerby and Rogers (2005), Johansen and Jackson (2004)]. These X-rays based methods are non-destructive, impassive, rapid and highly accurate. The X-ray/γ-ray transmission methods are suitable for bulk analysis and require an accurate measurement of the sample thickness and a good geometrical arrangement. Recently, Upmanyu *et al*. [2021] has reported a method to determine thickness of C_{60} layer prepared on the glass substrate by measuring absorption of the characteristic X-rays of Si present in the substrate.

In a general experiment involving irradiation of a sample by monoenergetic photons, the resulting spectrum consists of characteristic x-ray peaks from different elements present in a sample, an elastic-scattered peak and an inelastic-scattered peak. An element with concentration, m, in a sample is related to N counts/s under the characteristic x-ray peak or to a contribution of N counts/s under the elastic- or inelastic-scattered peak by the relation

$$m = \frac{N}{I_o G \sigma \varepsilon \beta} \quad (1)$$

where I_oG is intensity of the incident photons falling on the portion of target visible to the detector, ε is efficiency of the detector at the corresponding energy, and σ is the corresponding interaction cross section. β is the absorption correction factor that accounts for absorption of the incident and the emitted/scattered photons in the target and the product $m\beta$ represents the effective thickness of the target for a set of incident and emitted photon energies under consideration.

In case all the elements present in the sample emit fluorescent X-rays which are detectable by semiconductor detectors, one can make use of the X-rays to determine their concentration and hence, thickness of different layers in a multilayer sample can be determined. This method of measurement of characteristic X-rays from the sample using semiconductor detectors, popularly known as energy dispersive x-ray fluorescence (EDXRF) technique [Vogt and Dargel (2005), Carapella *et al*. (2007), Queralt *et al*. (2010), Mahajan *et al*. (2018), Tiwary *et al*. (2019)], has been well established to determine the elemental concentrations of various elements simultaneously. The EDXRF technique cannot be used for elements whose characteristic X-rays are not detectable by these detectors. The important modes of photon interaction with matter, *viz*., elastic and inelastic scattering also have applications in such characterization [Vogt and Schramm (1999), Martinez *et al*. (2000)]. The scattering measurements are particularly useful for elemental analysis of environmental, biological and geological samples with a major part of the matrix consisting of low-Z elements, which do not produce easily detectable x-rays for analysis by EDXRF technique [Macfarlane *et al*. (2003)]. The elastic-scattering measurements in the x-ray energy region, i.e., below 100 keV, are used for Z-dependent characterization of materials, while the inelastic-scattered x-rays are used for measurements of several physical quantities such as electron density, target mass and mass density. For measuring thickness of the low-Z sample or a sample with low-Z material used as coating and/ or backing on a high- Z substrate, one can preferably make use of information related to elastic- and inelastic-scattered photons. In this method, the analytical data can be deduced from the x-ray spectra simultaneously.

In the present work, the analytical methods based on the information of fluorescent x-rays, the elastic and inelastic scattered photons by the sample have been used to determine thickness of (a) polymer films by measuring the inelastic-scattered photons and (b) different layers of multilayer samples consisting of high-Z elemental/alloy-foil sandwiched between polymer films.

MATERIAL AND METHODS

The geometrical arrangement used for the photon-atom interaction measurements is shown in Fig. 1. It consisted of the exciter system NER-496 (New England Nuclear, USA) and an annular source of ^{241}Am (300 mCi, procured from DUPONT, USA). The source is in the form of a circular flat ribbon of 30-mm diameter and 4 mm width. The 59.5 keV γ-ray photons, emitted from the ^{241}Am source with probability = 35.6 per 100 decays [Browne *et al.* (1986)], were made to scatter from different targets through an angle of 120^o. An Si(Li) detector (28.27 mm^2 x 5.5 mm, FWHM = 180 eV at 5.89 keV and 400 eV at 59.5 keV), with a 3-mm-diam Pb-collimator, was used to detect the scattered and fluorescent radiations from the target. The whole arrangement resulted in smooth background in the region of the elastic- and inelastic-scattered peaks. The geometrical setup involving ^{241}Am annular source was optimized for measurements involving few mm-thick targets of low-Z materials. A detector collimator of 7-mm diameter has been used in the setup. The count rate is observed to be constant within 2% over a target-detector distance of ~5mm. In view this, the measurements with few mm thick low-Z targets can be done to a reasonable approximation without any correction to the incident photon intensity (I_o) and detector efficiency (ε) product [Eqn. (1)].

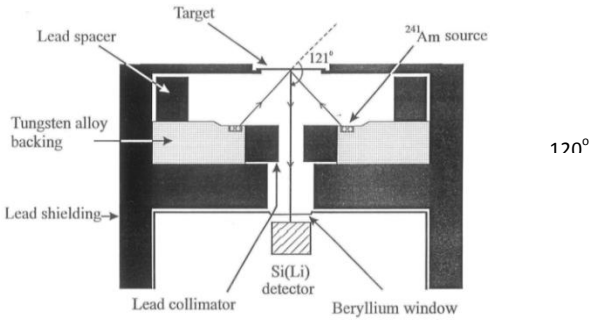

Figure 1: Target, source and detector geometrical arrangement used in the present measurements.

RESULTS

A. Measurement of thickness of polymer films

The information about the inelastic-scattered peak has been used to measure thickness of polypropylene films [$(C_3H_6)_n$, density = 0.855 g/cm^3]. The spectra of the polypropylene films were taken using the geometrical setup shown in Fig. 1. The spectrum, shown in Fig. 2, mainly consists of the inelastic-scattered peak of energy 50.6 keV corresponding to scattering angle of 120^o. For the present set up in reflection geometry, the absorption correction factor (β) [Sharma *et al*. (2008)], is given by

$$\beta = \frac{1-\left[exp(-1)\left(\frac{\mu_1}{cos\,\theta_1}+\frac{\mu_2}{cos\,\theta_2}\right)m\right]}{\left(\frac{\mu_1}{cos\,\theta_1}+\frac{\mu_2}{cos\,\theta_2}\right)m} \quad (2)$$

where θ_1 = 60^o and θ_2 = 0^o are the angles made by the incident and the detected scattered photons with the normal to the target surface, respectively. μ_1 and μ_2 are the attenuation coefficients for the incident and the emitted/scattered photons in the sample and were deduced using interpolated values from Tables given by Storm and Israel (1970). The polypropylene film consists of low-Z elements, namely C and H, therefore, the photoelectric process contributes very little to the absorption. For the inelastic-scattering measurements, it has been suggested that one should use only the photoelectric part of the attenuation coefficient [Strom and Israel (1970)] in calculation of absorption correction β (Eqn. 2) [Shahi (2000), Shahi *et al*. (2001)]. Therefore, absorption correction β is found to be small even u[illegible] hickness of 600 mg/ cm^2 of polypropylene film. Spectra were taken for different number of polypropylene films each of thickness = 14.2 mg/cm^2 and area under the inelastic-scattered peak were determined. The graph between the inelastic-scattered peak count-rate and film-thickness is found to be linear as shown in Fig. 3. The elastic-scattered peak count rate is negligibly small ~5x10^{-4} cps/mg/cm^2. The background counts under the

inelastic-scattered peak were 1.42 counts/s compared with 40 counts/s for a 14.2 mg/cm^2 thick polypropylene film.

The same set up has been used to measure thickness of thin mylar films. Spectra were also taken for mylar films of different thickness for time duration 10,000 s. The graph between the inelastic-scattered peak count-rate and film-thickness was also found to be linear even upto 284 µg/cm^2, the lowest thickness measured in the present work. 6.23 counts/s were observed under the inelastic scattered peak for mylar film of thickness 1725 µg/cm^2, and 2.18 counts/s for the mylar film of thickness 284 µg/cm^2. The background counts under the inelastic-scattered peak in the setup were 1.42 counts/s. This means in a spectrum of duration 10,000 s taken for a 100 µg/cm^2 of mylar film, ~2500 counts will be contributed under the inelastic peak and a contribution of background of ~14200 counts. The film thickness can be determined with an error of ~7%. This method can be used for even lower mylar film thickness by reducing the background counts. This can be achieved using either a better shielding in the setup or using another photon source having lower background due to bremsstrahlung etc. Main advantage of this method is that one can calibrate the system with thicker fi1ms and use it safely to determine thickness of thin films of same material.

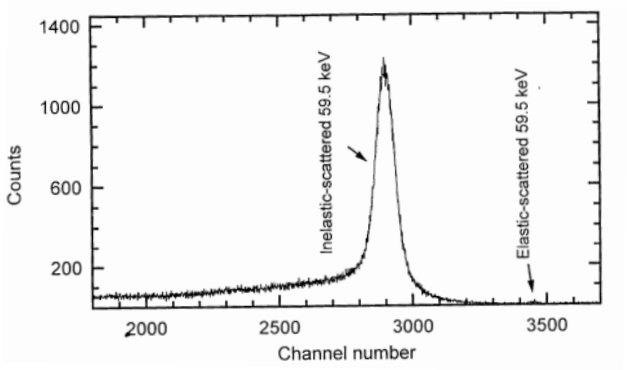

Figure 2: Spectrum of polypropylene film at 59.5 keV incident photon energy.

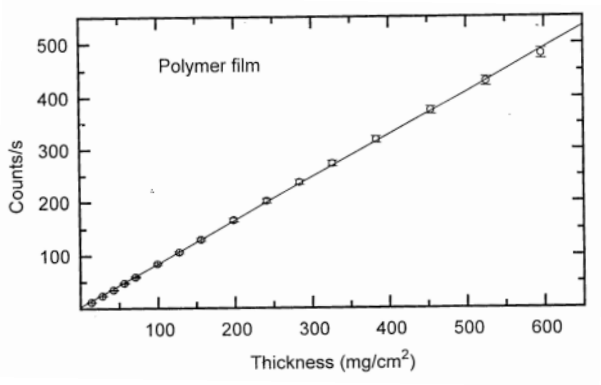

Figure 3: Inelastic-scattered peak area plotted as a function of thickness of polypropylene film. Error shown in the measured count rate is 2%.

B. Measurement of thickness of Mylar layer coated on a Cu-foil

For measurement of thickness of different layers in a sample consisting of Cu-foil coated with mylar film, spectra were taken for different number of films each of thickness = 14.2 mg/ cm^2 placed below a Cu foil of thickness 18.8 mg/cm^2. The spectrum, shown in Fig. 4, mainly consists of Cu K X-rays, inelastic- and elastic-scattered peaks. The graph between the inelastic-scattered peak count-rate and film-thickness, shown in Fig. 5, is found to be linear. Then, spectra were taken by placing different number of films above the Cu foil with the 5 films placed below the Cu foil. The graph between the inelastic-scattered peak count-rate and film-thickness (Fig. 5) for this case is also found to be linear. The elastic-scattered peak count rate is mainly contributed by the Cu foil and is found to be constant after correcting for the absorption in the film placed below it (Fig. 6). In a separate experiment, the absorption coefficients for the 59.5 keV photons in the film were measured and found to be 0.152 cm^2/gm.

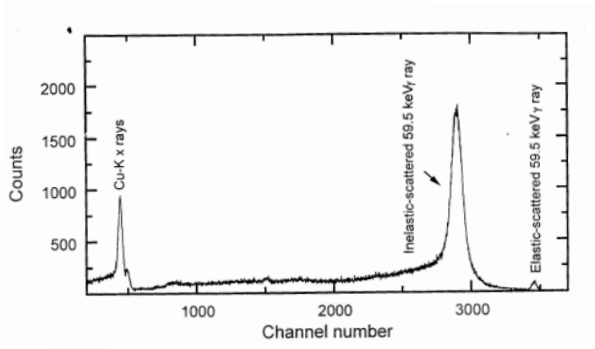

Figure 4: Spectrum of Cu foil sandwiched between polymer (Mylar) films taken using 59.5-keV photon incident on it.

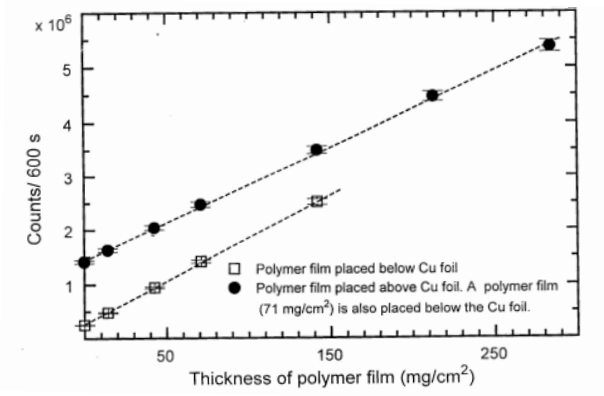

Figure 5: Inelastic-scattered peak count rate plotted as a function of thickness of polymer (Mylar) film placed below and above the Cu foil (18.8 mg/cm^2). Error shown in the measured count rate is 2%.

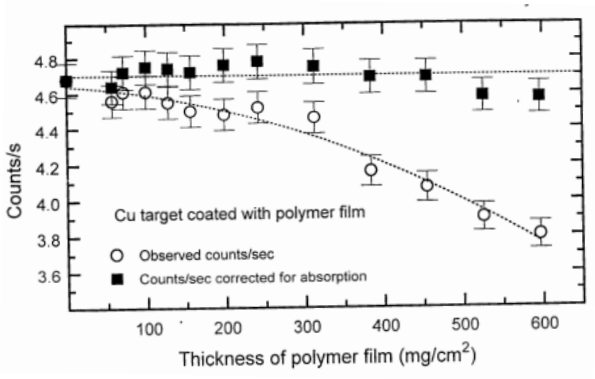

Figure 6: Elastic-scattered peak count rate plotted as a function of thickness of polymer (Mylar) film placed below the Cu foil. Error shown in measured count rate is 2%.

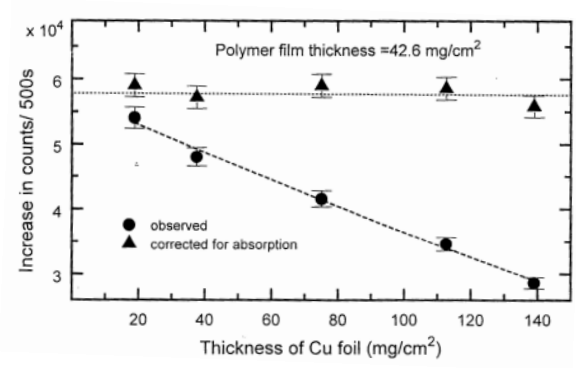

Figure 7: Increase in counts/500s under the inelastic-scattered peak on placing polymer (mylar) film (42.6 mg/cm^2) above Cu-foil plotted as a function of Cu-foil thickness.

C. Measurement of thickness of different layers in a sample consisting of Cu-foil sandwiched between Mylar films

A sample consisting of a Cu-foil sandwiched between two Mylar films of equal thickness was analyzed for determination of thickness of the Cu foil and the Mylar films. The 59.5-keV photons emitted from ^{241}Am were made incident on the sample in the geometrical setup shown in Fig. 1. The spectrum of sample consists of peaks corresponding to characteristic K x-rays of Cu, elastic-scattered and inelastic-scattered 59.5-keV photons. Spectra were taken for (a) the sample and (b) the sample with an additional Cu foil placed above it. An increase in the count rate under the peaks corresponding to the elastic- and inelastic-scattered photons was observed in the spectrum (b) than that in the spectrum (a). This indicates that the sample is not infinite thick for these photons. Therefore, the information of elastic- and inelastic-scattered photons can be used in the determination of thickness of different layers. Another, set of spectra were taken for (a) the sample, (b) the sample with a mylar film of known thickness placed below it, (c) the sample with a Mylar film of known thickness placed above it, and (d) pure Cu target of known thickness. The measured

absorption coefficient for the 59.5-keV photons in the mylar film (0.152 cm^2/gm) indicates only small absorption of 59.5-keV photons in the mylar film in the sample. Spectra were analyzed to determine counts/ s under the peaks corresponding to inelastic-arid elastic-scattered 59.5-keV photons. From the spectrum (d) the $I_oG\varepsilon\sigma$ product was determined using Eq. (3) for elastic- and inelastic-scattered photons in case of Cu.

$$I_o G \sigma_i \varepsilon_i = \frac{N_i}{m_i \beta_i} \quad (3)$$

The mylar films contribute mainly to the inelastic-scattered peak only. For the initial analysis the absorption in the Mylar films was ignored. The count rate under the elastic-scattered peak in the spectrum (a) was used in the Eq. (3) for first estimation of m_{cu}, i.e., assuming that the elastic-scattered peak is only due to Cu present in the sample. For this thickness of Cu foil, the inelastic-scattered peak counts were estimated using Eq. (3). These counts were subtracted from the observed counts under the inelastic-scattered peak in the spectrum (a) to get contribution of the Mylar films $N_{myl\text{-}inel}$. Total thickness of the Mylar film in the sample was evaluated usi the relation (taking equal thickness of both Mylar layers of the sample)

$$m_{poly} = \frac{N_{myl-inel}}{N_{myl-inel}^{above} + N_{myl-inel}^{below}} \quad (4)$$

where $N_{myl-inel}^{below}$ and $N_{myl-inel}^{above}$ are increase in count rate/ unit thickness ur 'the inelastic-scattered peak due to Mylar of known thickness placed below and above the sample, respectively. These were determined by subtracting the count rate under the inelastic- scattered peak from spectrum (a) from that in the spectra (b) and (c), respectively.

The whole analysis was repeated after correction for small absorption of the elastic-scattered photons in the Mylar film and considering the contribution of Mylar film to the elastic-scattered peak (5 x 10^{-4} counts/s/mg) in the spectrum (a). The results obtained were m_{Cu} = 34.4 mg/cm^2 and m_{poly} =138 mg/cm^2 which agree well with the actual values m_{cu} = 34.2 mg/cm^2 and m_{poly} = 142 mg/cm^2 determined by weighing method. The above procedure can be extended for Cu foil of thickness ~ 10 μg/cm^2 and also to the Cu foil sandwiched between unequal thickness of Mylar films.

D. Elemental analysis of binary Pb-Sn alloy

The quantitative elemental analysis of the Pb-Sn binary alloy sample was done in the geometrical set up shown in Fig. 1. The detected spectrum taken using Si(Li) detector is shown in Fig. 8. It shows peaks corresponding to Pb Lγ x rays, Sn K x rays, and elastic- and inelastic- scattered photons. The escape peak corresponding to Sn K x rays is seen to overlap the Pb Lγ x ray peak. Spectra were also taken using targets of pure Pb and Sn of thickness 314 mg/cm^2 and 400 mg/cm^2, respectively, in the same geometrical set up.

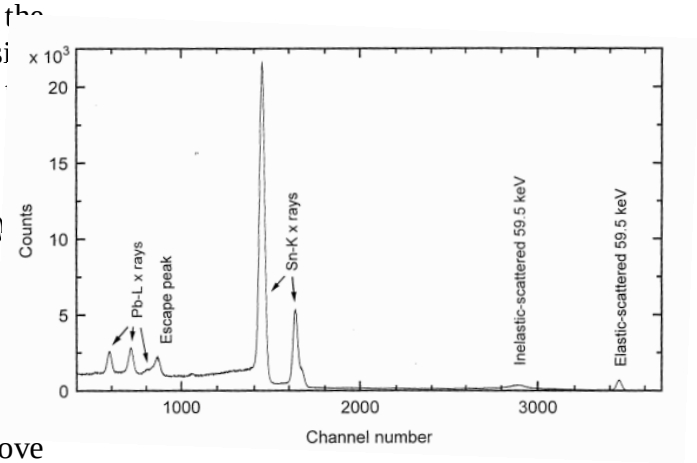

Figure 8: Spectrum of sample consisting of Pb-Sn foil taken using 59.5 keV photons incident on it.

The spectra were analysed for areas under the elastic-scattered 59.5-keV peak. The scattering

angle has been determined from the energy-shift of the inelastic-scattered peak from the elastic-scattered peak. These count rate from spectra of pure Pb and Sn targets were used in Eq. (3) to determine the $I_oG\varepsilon\sigma$ factor for elastic-scattered photons for respective elements. Since $I_oG\varepsilon$ factor is same for the elastic-scattering measurements in case of Pb-Sn alloy, a graph is plotted for expected counts under the elastic-scattered peak, $N_{Pb-Sn}^{expecte\ d}$, for different fractions *x* of Pb in Pb-Sn alloy using the expression.

$$N_{Pb-Sn}^{expected} = \frac{I_o G\varepsilon[x\,\sigma_{Sn} + (1-x)\sigma_{Pb}]}{(m\beta)_{Pb-Sn}} \qquad (5)$$

The value of x = 0.582 corresponding to the measured count rate under in the elastic-scattered peak in the Pb-Sn alloy spectrum gives the composition of the alloy (Fig. 9).

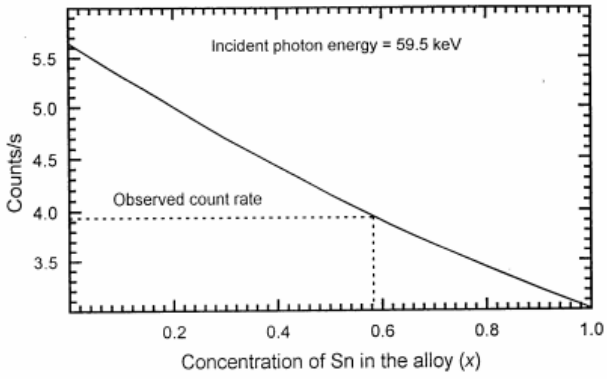

Figure 9: The expected counts/s under the 59.5 keV elastic-scattered peak plotted as a function of concentration of Sn in the alloy.

E. Measurement of composition and thickness of foil of Pb-Sn alloy sandwiched between polymer films

A sample consisting of a foil of Pb-Sn alloy sandwiched between two polymer films of equal thickness was analysed for determination of thickness and composition of foil of Pb- Sn alloy and thickness of the polymer film coating. The 59.5-keV photons emitted from ^{241}Am were made incident on the sample in the geometrical set up shown in Fig. 1. The spectrum of sample consists of peaks corresponding to characteristic L x rays of Pb and K x rays of Sn, elastic-scattered and inelastic-scattered 59.5- keV photons, which is similar to that shown in Fig. 8.

Spectra were taken for (a) the sample, (b) the sample with an additional Pb foil placed above it, and (c) the sample with an additional Sn foil placed above it. No increase in the count rate of the Pb L x rays was observed in the spectrum (b) than that in the spectrum (a). This indicates that the sample was infinite thick for the Pb L x rays. However, an increase in the count rate of the Sn K x rays was observed in the spectrum (c) than that in the spectrum (a), indicating the sample is not infinite thick for Sn K x rays. Therefore, Sn K x rays can be used in the determination of thickness of foil of Pb-Sn alloy.

Another, set of spectra were taken for (a) the sample, (b) the sample with a polymer film of known thickness placed below it, (c) the sample with a polymer film of known thickness placed above it, (d) pure Sn target of known thickness, and (e) pure Pb target of known thickness. In a separate experiment, the absorption coefficients for 25.8-keV (Sn-K x rays), 42.8-keV (Gd-K x rays), 59.5-keV photons in the polymer film were measured and were found to be 0.205, 0.183 and 0.152 cm^2/gm, respectively. This indicates only a few percent absorption of Sn-K x rays and scattered 59.5-keV photons in the polymer film coated on the sample. Spectra were analysed to determine counts/s under the peaks corresponding to inelastic- and elastic-scattered 59.5-keV photons, and Sn-K x rays. From the spectra (d) and (e), the $I_oG\varepsilon\sigma$ product was determined using the Eq. (3) for elastic- and inelastic-scattered photons in ease of Pb, and K x rays, elastic- and inelastic-scattered photons in case of Sn. The polymer films contribute mainly to the inelastic-scattered

peak. For the initial analysis the absorption in the polymer films was ignored. Iteration method as discussed below was used for analysis.

Step I: The count rate under the elastic-scattered peak in the spectrum (a) was used in the Eq. (3) for first estimation of m_{pb}, *i.e.*, assuming that the- elastic-scattered peak is due to the sample consisting of Pb only. The count rate under the Sn-K x-ray peak in the spectrum (a) was used in Eq. (3) with $\beta = 1$ for first estimation of m_{Sn}, *i.e.*, Sn present in the sample.

Step II : Taking the composition of Pb-Sn alloy estimated in Step I, next estimation of os was done by using Eq. (5) with, β calculated for this composition of alloy Eq. (2)**.**

Step III : For the composition of alloy estimated in Step II, the count- rate under the elastic-scattered peak was estimated using Eq. (5). Keeping the m_{pb} : m_{Sn} in the sample to be the same, the total thickness of the sample was normalized to give estimated count rate to be equal to the measured one.

Steps II and III were repeated five times to get converging values to be m_{Sn} = 34.4 mg/cm^2 and m_{Pb} = 34.4 mg/cm^2. For this composition of Pb-Sn alloy, the inelastic-scattered peak counts/s were estimated using Eq. (5). These counts were subtracted from the observed counts under the inelastic-scattered peak in the spectrum (a) to get contribution of the polymer films . Total thickness of the polymer film was evaluated using the Eq. (4). The $N_{poly-inel}^{below}$ and $N_{poly-inel}^{above}$, were determined by subtracting the count rate under the inelastic-scattered peak from spectrum (a) from that in the spectra (b) and (c), respectively. The contribution of sum peak of Sn K x rays to the inelastic-scattered peak was estimated and subtracted. The whole analysis was repeated after correction for small absorption of Sn-K x rays and elastic-scattered photons in the polymer film and considering the contribution of polymer film to the elastic-scattered peak in the spectrum (a). The results obtained were mass of Sn in the sandwiched alloy foil use m_{Sn} = 35.8 mg/cm^2, m_{Pb} = 22.9 mg/cm^2 and m_{Poly} = 137 mg/cm^2 which agree well with the total thickness of the alloy foil m_{alloy} = 58. 0 mg/cm^2 and m_{poly} = 142 mg/cm^2.

DISCUSSION

In the present work, the information of fluorescent x-rays, the elastic and inelastic scattered photons have been used for sample analysis. In case of low-Z polymer films where fluorescent X-rays are not detectable by semiconductor detectors, thickness is deduced by measuring the photons inelastic-scattered by the film. It is demonstrated that the inelastic-scattering measurements in the present setup can be used to measure thickness of Mylar films over a wide range 100 µg/cm^2 – 600 mg/cm^2. The setup can be further improved to reduce background for measurements in case of Mylar films of lower thickness. The characteristic X-ray, and inelastic- and elastic-scattering information has been used to measure thickness of different layers of samples consisting of Cu-foil sandwiched between Mylar films, and to determine composition of sandwiched foil of Pb-Sn alloy. Because of very low absorption effects in low-Z materials, *e.g.*, polymer films, one can make use of relatively thicker samples to calibrate the system and use it to measure very low thickness. For the measurements of lower thickness of the polymer films, the lower-energy X rays can be used. The required low-energy photons of desired energy can be obtained by exciting K x-rays of a suitable secondary exciter excited by the 59.5 keV photons from the available ^{241}Am source [Alrakabi *et al*. (2013)]. Unlike the fluorescent x-ray spectrum, the scattering of monoenergetic incident photons from different elements present in the sample results in only one peak each for the elastic- and inelastic-scattered incident photons. Hence, elemental analysis using scattered peak information can be done only if different elements have widely different scattering cross sections.

In case of all the elements present in the sample emit fluorescent X-rays detectable by semiconductor detectors, one can make use of the X-rays to determine concentration of these elements in the sample and hence, thickness of the sample using EDXRF technique. However, for measuring thickness of the low-Z sample or a sample with low-Z material used as coating and/ or backing on a high- Z substrate, one can preferably make use of information related to elastic- and inelastic-scattered photons, which is available in the spectrum along with the fluorescent X-rays of the elements present in the samples. Also, the absorption of the detectable X-rays, emitted by the back layer of the sample, in the front layer can be used for front layer thickness determination [Upmanyu *et al*. (2021)].

The inelastic- and elastic-scattering cross sections (cm^2/gm) for the 59.5-keV (γ-ray from decay of ^{241}Am) incident photons at an angle of 120° are plotted as a function of atomic number (Z), in Figs. 10 and 11, respectively. It is clear from Fig. 10 that the inelastic-scattering cross sections do not vary significantly as a function of Z and hence, cannot be exploited much for identification of elements in samples. However, because of this property the inelastic-scattered peak information can be used to monitor the thickness of samples having same major matrix and with other elements present in traces only. In the analysis of treated and untreated biological samples in pellet form using EDXRF technique, the error due to non-uniformity in thickness of pellet can be minimized by with the help of the area under the inelastic-scattered peak which itself is proportional to the thickness of the sample portion contributing to the detected x-ray spectrum. This will reduce error in determination of concentrations of trace elements and hence a better resolution for the treated and untreated samples.

The other important observation from Fig. 10 is that the inelastic-scattering cross section (cm^2/g) in H is higher by a factor of ~2 as compared to that for other elements. This is because mass of the atom is mainly contributed by the nucleons and scattering is mainly due to the electrons. For H, the ratio of number of electrons to number of nucleons is very different from the other elements. Hence, the information of inelastic-scattered photons can be exploited to estimate abundance of H in hydrogen-rich samples [Shahi (2000)].

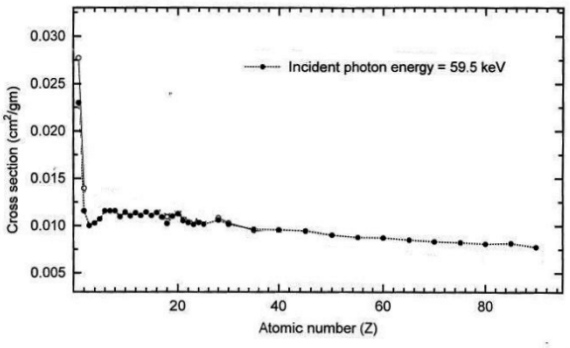

Figure 10: Theoretical calculated inelastic-scattering cross sections (cm^2/gm) [Hubbell (1975,1977)] for the 59.5-keV incident photons at an angle of 120° as a function of atomic number (Z).

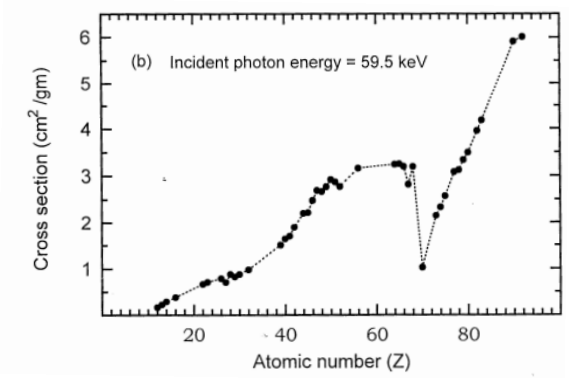

Figure 11: Theoretical elastic-scattering cross sections (cm^2/gm) [Kissel *et al.* (1995), Kissel (2000)] for the 59.5 keV photons at 120° angle as a function of atomic number.

The elastic-scattering cross sections at 59.5 keV (Fig. 11) vary considerably as a function of Z upto Z ~ 50. Thereafter, these remain nearly constant and exhibit considerable

decrease for the elements having absorption edge in the vicinity of incident photon energy, and again increase considerably for higher-Z elements. So, the elastic-scattering information can be used for elemental analysis of alloys with constituent elements having widely different elastic-scattering cross sections.

CONCLUSIONS

An X-ray inelastic scattering method has been proposed for determination of thin film thicknesses. The method is extended to determine thicknesses of low-Z organic film coated on metal layers. This methodology can also be developed for portable EDXRF spectrometer equipped with Peltier-cooled detector and air-cooled low-power X-ray tube for many field applications. Various aspects of elemental analysis of samples using information available in as EDXRF experiment, i.e., about characteristic X-rays, elastic- and inelastic-scattered photons have been discussed. The inelastic scattering cross sections exhibit small variation with atomic number and therefore, inelastic-scattering measurements are used to determine thickness of samples having same major matrix and with other elements present in traces only. Main advantage of this method is that one can calibrate the system with thicker low-Z (polymer) fi1ms and use it safely to determine thickness of thin films of same material. The elastic scattering cross sections exhibit significant variation with atomic number, which makes elastic scattering measurements useful for elemental analysis of alloys with elements are present as major constituents and have having widely different elastic-scattering cross sections.

ACKNOWLEDGEMENT

Financial supports from the University Grants Commission (UGC), New Delhi, for the Centre of Advanced Study (CAS) in Physics grant and Department of Science and Technology (DST) for FIST grant are duly acknowledged.

REFERENCES

Alrakabi, M., Kumar, S., Sharma, V., Singh, G. and Mehta, D. 2013. Alignment of L_3 subshell vacancy states in Au, Bi, Th and U following photoionisation and effect of external magnetic field, Eur. Phys. J. D 67: 99 (8 pages).

Browne, E., Firestone, R.B. and Shirley, V.S. (Eds.). 1986. Table of Radioactive Isotopes, Wiley, New York.

Carapelle, A. , Fleury-Frenette, K., Collette, J.P., Garnir, H.P. and Harlet, P. 2007. Portable X-ray fluorescence spectrometer for coating thickness measurement, Rev. Sci. Instrum. 78: 123-125.

Draxler, M., Zoister, S., Kastner, F., Bergsmann, H. and Bauer, P. 2002. Characterization of ultrathin Cr layers on PET by RBS and XRF, Surf. Interface Anal. 34: 763-766.

Ebel, M.F., Svagera, R., Lindner, M., Praxmarer, N., Hager, C. and Ebel, H. 1999. Investigations of thin layers by TEY, XRF, EPMA and XPS - a comparison of X-ray analytical methods, Adv. X Ray Anal. 41: 62-75.

Gardner, R. P., Metwally, W. A. and Shehata, A. 2004. A semi-empirical model for a ^{90}Sr beta-particle transmission thickness gauge for aluminum alloys, Nucl. Instrum. Methods B 213: 357-363.

Hobbis, A. and Aruleswaran, A. 2005. Non-contact thickness gauging of aluminium strip using EMAT technology. Springer Series in Measurement Science and Technology, Huang, S. and Wang, S., New Technologies in Electromagnetic Non-Destructive Testing, *Nondestr*. *Test*. *Eval*. *20*(4): *211*–220.

Hubbell, J.H., Veigele, W.J., Briggs, E.A., Brown, R.T., Cromer, D.T., Howerton, R.J. 1975. Atomic form factors, incoherent scattering functions, and photon scattering cross sections, J. Phys. Chem. Ref. Data 4: 471, *ibid* 1977. J. Phys. Chem. Ref. Data 6: 615(E).

Hussein, E. M. A. 2003. Handbook on Radiation Probing, Gauging, Imaging, and Analysis, Kluwer Academic Publishers, Dordrecht.

Johansen, G. A. and Jackson, P. 2004. Radioisotope gauges for industrial process measurements, John Wiley and Sons, Ltd., https://doi.org/10.1002/0470021098.

Kissel, L., Zhou, B., Roy, S.C., Sen Gupta, S.K. and Pratt, R.H. 1995. The validity of form-factor, modified-form-factor and anomalous-scattering-factor approximations in elastic scattering calculations, Acta Cryst. A. 51: 271.

Kissel, L. 2000. Radiat. Phys. Chem., 59: 185-200.

Lhotka, J., Kuzel, R., Capuccio, G. and Valvoda, D. 2001. Thickness determination of thin polycrystalline film by grazing incidence X-ray diffraction, Surf. Coat. Technol.184: 95–100.

Mahajan, R., Abhilash, S.R. , Sharma, P. , Kaur, G., Kabiraj, D., Duggal, H., Mehta, D. and Behera, B. R. 2018. Thin targets for nuclear reaction studies using NAND facility, Vacuum 150: 203-206.

Martinez V.D., Hidalgo M. and Barrea, R.A. 2000. X-ray fluorescence analysis by the fundamental parameters method without explicit knowledge of the excitation beam spectrum, X- ray Spectrometry 29: 245-248.

Mcfarlane, N. J. B., Speller, R.D., Bull, C. R. and Tillett, R. D. 2003. Detection of Bone Fragments in Chicken Meat using X-ray Backscatter , Biosystems Engineering 85(2):185-199

Molt K. and Schramm, R. 1999. Determination of light elements in organic liquid matrices by principal component regression in EDXRS using backscattered radiation, X-ray Spectrometry 28: 59-63.

Rajesh, K. K., Musthafa, M. M., Hosamani, M. M., Shamlath, A., Abhilash, S. R.

and Kabiraj, D. 2017. Fabrication of carbon sandwiched thin targets of ^{138}Ba by evaporation, Technique, Vacuum 141: 230-234.

Ribeiro, J. M. , Correia, F. C., Salvador, P. B., Rebouta, L., Alves, L. C., Alves, E., Barradas, N. P., Mendes, A. and Tavares, C.J. 2019. Compositional analysis by RBS, XPS and EDX of ZnO: Al,Bi and ZnO:Ga, Bi thin films deposited by d.c. magnetron sputtering, Vacuum 161: 268-275.

Shahi, J.S., Kumar, A., Mehta, D., Puri, S., Garg, M. L. and Singh, N. 2001. Inelastic scattering of 59.54 keV photons by elements with $13 \leq Z \leq 82$, Nucl. Instr. And Meth. B 179: 15-23.

Shahi, J.S., Ph.D. 2000. Thesis, X-ray Photon Scattering cross section measurements and application in Elemental Analysis using EDXRF technique, Panjab University, India.

Sharma, V., Kumar, S., Mehta, D. and Singh, N. 2008. L-subshell vacancy decay processes for elements with $52 \leq Z \leq 57$ following ionization using Mn Kα x rays Phys. Rev. 78: 012507.

Sowerby, B. D. and Rogers, C.A. 2005. Gamma-ray density and thickness gauges using ultra-low activity radioisotope sources, Appl. Radiat. Isot. 63: 789-793.

Storm, E. and Israel, H.I. 1970. Photon cross sections from 1 keV to 100 MeV for elements Z=1 to Z=100, Nucl. Data Tables 7: 565-681.

Suzukia, K., Tsuchiya, B., Yasuda, K. and Nakata Y., 2020. Light element analysis of ceramics using in-air ERDA and TOF-ERDA, Nucl. Intrum. Meth. B 478: 169-173.

Tiwary, S.S., Sharma, H.P., Chakraborty, S., Majumder, C., Singh, G., Mehta, D. , Kumar, S., Abhilash, S.R., Kabiraj, D., Singh, R.P. and Muralithar, S. 2019. Fabrication of isotopic ^{127}I target from potassium iodide for heavy ion nuclear reactions, Vacuum 167: 336-339.

Queralt, I., Ibañez, J. , Marguí, E. and Pujol, J. 2010, Thickness measurement of

semiconductor thin films by energy dispersive X-ray fluorescence benchtop instrumentation: Application to GaN epilayers grown by molecular beam epitaxy, Spectrochimica Acta Part B 65: 583–586.

Upmanyu, A. K., Kailash, Kapil, A. , Mehta, D. and Kumar, S. 2021. Thickness measurement of low-Z films fabricated on thick substrate using EDXRF technique Vacuum 183: 109852 (6 pages).

Vogt, C. and Dargel, R. 2005. Determination of layer thickness with μXRF, Appl. Surf. Sci. 252: 53-56.